Received: September 6, 2025; **Accepted:** November 2, 2025; **Published:** January 1, 2026.
DOI. 10.30473/coam.2025.75850.1343
Volume 11, Issue 1, p.p. 73-99: Winter-Spring (2026)
Research Article

Open Access

Control and Optimization in Applied Mathematics - COAM

Optimal Harvesting of Three Species Intraguild Predation Model with Ratio-dependent Functional Response

Subramani Magudeeswaran[1], **Muthuradhinam Sivabalan**[2], **Mehmet Yavuz**[3,4] ✉, **Dharmendra Kumar Singh**[5], **Kannimuthu Giridharan**[1]

[1] Department of Mathematics, Sree Saraswathi Thyagaraja College, Pollachi, Tamilnadu, India
[2] Department of Mathematics, Sri Ramakrishna Mission Vidyalaya College of Arts and Science, Coimbatore, Tamilnadu, India
[3] Department of Mathematics and Computer Sciences, Faculty of Science, Necmettin Erbakan University, 42090 Konya, Turkiye
[4] Department of Applied Mathematics and Informatics, Kyrgyz-Turkish Manas University, Bishkek 720038, Kyrgyzstan
[5] Department of Mathematics, School of Basic Sciences, CSJM University, Kanpur, India.

✉ **Correspondence:**
Mehmet Yavuz
E-mail:
mehmetyavuz@erbakan.edu.tr

How to Cite
Magudeeswaran, S. Sivabalan, M., Yavuz, M., Kumar, Singh, D., Giridharan, K. (2026). "Optimal harvesting of three species intraguild predation model with ratio-dependent functional response", Control and Optimization in Applied Mathematics, 11(1): 73-99, doi: 10.30473/coam.2025.75850.1343.

Abstract. In this study, we fabricate and investigate a three-species intraguild predation model with a ratio-dependent functional response. We also incorporate harvesting efforts into both intraguild prey and intraguild predators. Then, we analyze the dynamical behavior of the proposed model by taking the harvesting rate as the bifurcation parameter. We precisely outline the prerequisites for the proposed model's existence, stability, and bifurcation near the equilibrium points. It contributes to a better understanding of the impacts of harvesting on the survival or extinction of one or more species in the proposed model. Furthermore, we derive the suggested model's bionomic equilibrium and optimum harvesting policy by using the *Pontryagin's maximum principle*. Finally, we provide some numerical simulations to validate the analytical results. In addition, we give some graphical representations to validate our results.

Keywords. Local stability, Hopf-bifurcation, Intraguild predation, Optimal harvesting.

MSC. 37C75; 34C23.

1 Introduction

There are many issues that are biologically interesting in our environment that require a substantial understanding of the critical behavior and intrinsic nature of mathematical modeling. Instead of calculating the change in a particular population , the main objective of the model's development is to examine how complex it is in an ecosystem. Mathematical modeling of predator and prey population dynamics has emerged as an excellent research topic in the field of mathematical ecology. Model-based studies of ecological problems were first developed by Lotka and Volterra [28, 49]. In the Lotka-Volterra model [46], the predator population depends on the number of prey. This situation is not considered when there is a scarcity of prey and the predator must look for new prey. In the investigation of the interaction of population dynamics, a functional response plays an essential role in it, and the functional response is the consumption rate of the predator as given by a function of prey density. There are numerous types of functional responses effectively acting in population dynamics, they are Holling type I, II, and III [13, 23, 30, 35, 48], Crowley-Martin [12, 47], Hassell-Varley [22], Beddington [6] and ratio-dependent [4, 43].

The management of renewable resources, such as fisheries and forests, through science is the focus of bioeconomic modeling. In recent times, the mathematical modeling of prey-predator models has grown to be an extremely fascinating field of study for many economists, mathematicians, and ecologists. Due to its significance, the issue of optimal harvesting in predator-prey systems rules both ecology and bioeconomics. On the basis of Clark's [10] demonstration of the concept of optimal equilibrium for the combined harvest of two distinct species, other authors have created their own models. In the absence of a harvest, each population adheres to a logistic growth law, whose yield level is proportionate to both its share level and harvest effort. The population then manages to deliver more benefits and the population remains stable. Jana et al. [24] discussed the two-dimensional prey-predator system, allowing for prey refuge and harvesting in the prey species only. There are numerous works related to the effect of harvesting on predator-prey interactions, the predator-prey model with selective harvesting on prey was discussed in [8, 14, 16, 21, 26, 29, 34, 36, 38, 44]. The selective harvesting of predators has been studied in [9, 45], and the selective harvesting effect for both species was investigated in [1, 5]. The authors in [20] explored the impact of harvesting in the tri-trophic food chain model and, importantly, discussed the existence of maximum sustainable yield when the top predator is harvested. Safuan et al. investigated a predator-prey model in an environment enriched by a biotic resource [41].

The food chain model of a two-species population in the context of shared biological resources is studied by Safuan et al. [40]. They analyzed the model, showing that during competition, death occurs between competitors. It plays an important role in shaping ecological communities. Intraguild predation is also known as exploitation competition or interference competition. Aside from the fact that both species face the harvesting process, they must compete to gain shared resources. In [19], the optimal harvest of an intraguild predation model with varying carrying capacities has been explored. The authors came to the conclusion that the enrichment parameter has a significant influence on the dynamics of prey, predation, and resources. The intraguild model's low, moderate, and high concentrations give diverse natures such as co-existence, destruction, and limit cycle. Collera and Balilo [11] discussed the dynamics of an intraguild predation model with linear harvesting on three species. The authors in [1] studied two species that compete for shared biological resources in the environment with harvesting effects.

Further, the authors concluded that the harvesting parameter plays a vital role in the ecosystem because harvesting activities reduce the population in an ecosystem. To prevent the extinction of the population, harvesting activities need to be controlled. In this sense the control strategies are essential. For example, Collera and Balilo [25] discussed the control mechanism for cancer-immune system interaction in an avascular environment. Mustapha et al. [32] developed a control strategy for the transmission dynamics of cholera. Different efficient control strategies were considered in the following studies: for corruption dynamics [2], for vector-borne infections [7], for chickenpox transmission dynamics [37], for carbon dioxide emissions [3], for Middle East respiratory syndrome transmission [17, 18], for HIV-1 model related to cancer cells [33], for a class of nonlinear affine systems [15].

Based on the preceding research investigations, we are encouraged to conduct the current study; we deal with exploitation strategies in an intraguild predation model with the ratio-dependent functional response, although this differs from earlier works in some basic assumptions.

The main contributions of this study are as follows:

- We develop a new intraguild predation (IGP) model with a ratio-dependent functional response, which more accurately reflects predator–prey interactions under limited encounter rates and interference—unlike most previous IGP harvesting models that use prey-dependent responses.
- We incorporate dual harvesting on both prey and predator populations, capturing realistic exploitation strategies. Previous studies typically harvest only one species or treat harvesting implicitly.
- We conduct a complete bioeconomic analysis by deriving the bionomic equilibrium, sustainable yield, profit function, and optimal harvesting policy under economic constraints—features rarely integrated into IGP systems.
- We identify complex dynamical behavior, including multiple local equilibria, transcritical and Hopf bifurcations, stability switches, and possible cycles, and we relate these mathematical outcomes to ecological mechanisms and management implications.
- We provide ecological and economic interpretations of all mathematical conditions, ensuring that stability results, threshold parameters, and bifurcation conditions are biologically meaningful for real-world resource management.

Also, we address the following concerns in this paper:

1. The factors might lead to the extinction of the species,
2. The factors encourage the coexistence of all three species,
3. Do both persist as a stable state or oscillations.

Further, we explore the possibilities of bionomic equilibrium and obtain the optimal principle of exploitation by using Pontryagin's maximum principle.

The rest of this paper is organized as follows: In Section 2, we formulate the three-species intraguild predation model with individual harvesting and ratio-dependent functional response. In Section 3 some needed preliminaries are discussed. in Section 4, we discuss the existence and local stability of the feasible equilibrium points. Bifurcation analysis for the constructed model is carried out in Section 5. The bionomic equilibrium and optimal harvesting of the proposed model are given in Section 6. We provide the numerical results in Section 7 and finally, we discuss and give the short conclusion of this paper in Section 8.

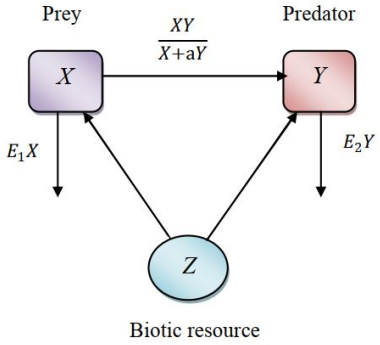

Figure 1: Schematic diagram of intraguild predation model

2 Model formulation

In this section, we propose the intraguild predation model with a ratio-dependent functional response and individual harvesting effects, which is an extension of the model proposed in Refs. [1, 19, 40, 41]. In [19], the authors studied the predator-prey model with variable carrying capacity and extended it with independent harvesting techniques as a possible extension of new inventions. The model is of the form:

$$\begin{aligned}
&\frac{dX}{dt} = c_1 X\left(1-\frac{X}{pZ}\right) - \alpha XY - E_1 X,\\
&\frac{dY}{dt} = c_2 Y\left(1-\frac{Y}{qZ}\right) + \beta XY - E_2 Y,\\
&\frac{dZ}{dt} = Z\left(c - uX - vY\right),\\
&X(0) = X_0 \geq 0, Y(0) = Y_0 \geq 0, \quad \text{and} \;\; Z(0) = Z_0 \geq 0.
\end{aligned} \tag{1}$$

In this paper, we extended the above model by considering that the predator consumes its prey in the form of a ratio-dependent type functional response. We formulate the model as follows:

$$\begin{aligned}
&\frac{dX}{dt} = c_1 X\left(1-\frac{X}{pZ}\right) - \frac{\alpha XY}{X+aY} - E_1 X,\\
&\frac{dY}{dt} = c_2 Y\left(1-\frac{Y}{qZ}\right) + \frac{\beta XY}{X+aY} - E_2 Y,\\
&\frac{dZ}{dt} = Z\left(c - uX - vY\right),\\
&X(0) = X_0 > 0, Y(0) = Y_0 > 0, \;\; \text{and} \;\; Z(0) = Z_0 > 0,
\end{aligned} \tag{2}$$

where parameters $\alpha, \beta, a, c, c_1, c_2, p, q, E_1, E_2, u$ and v are positive constants, X and Y be the size of prey and predator population, respectively, and Z be the size of biotic resources. The parameter a be the half-saturation constant, E_1 and E_2 are the independent harvesting effects of prey and predator, $c_i, (i = 1, 2)$ stands growth rates of prey and predator, respectively; pZ and qZ be the environmental carrying capacities of prey and predator, respectively. It is assumed that $0 < p < 1$ and $0 < q < 1$ with $p + q = 1$ so that $pZ + qZ$ (total carrying capacity). In our model, p and q represent the proportions of a shared limited resource allocated or utilized by two interacting species. The constraint $p + q = 1$ ensures that the entire available resource is partitioned between the two species, with no unused or "extra" resource. This reflects a biologically realistic scenario where resources are fully exploited in competitive

environments.The conditions $p, q \in (0,1)$ exclude trivial or ecologically unrealistic cases of exclusive monopolization(e.g., $p = 1, q = 0$) or no resource use. Thus, the model focuses on partial resource sharing, which is central in ecological theories of niche partitioning and coexistence. If $p > q$, the population of prey gets a larger proportion of biotic resources, resulting in a greater carrying capacity. That means prey can grow more than predators. Biotic resources with growth rate c are absorbed respectively by prey and predator for αX and βY, with u and v being constant. Because Z is a biotic resource, rises or reduces in its size could affect one or both prey and predator populations. The constants α and β stand for the capturing rate and the conversion rate of the consumed prey to predator, respectively.

To simplify the dynamical analysis and facilitate interpretation of the results, we nondimensionalize the model system (2) using the following transformation: $X \to \frac{xc_1}{q}, Y \to \frac{yc_1}{aq}, Z \to \frac{zc_1}{aq}, t \to \frac{t}{c_1}$, then the model (2) reduces the following form

$$\begin{aligned} \frac{dx}{dt} &= x\left(1 - \frac{x}{z}\right) - \frac{a_1 xy}{x+y} - h_1 x, \\ \frac{dy}{dt} &= r_1 y\left(1 - \frac{\gamma y}{z}\right) + \frac{a_2 xy}{x+y} - h_2 y, \\ \frac{dz}{dt} &= z\left(l - mx - ny\right), \end{aligned} \tag{3}$$

where $a_1 = \frac{\alpha c_1}{aq}, h_1 = \frac{E_1 c_1}{q}, r_1 = \frac{c_2}{c_1}, \gamma = \frac{1}{q}, a_2 = \frac{c_1 \beta}{aq}, h_2 = \frac{E_2 c_1}{aq}, l = \frac{c}{c_1}, m = \frac{u}{p}$ and $n = \frac{v}{pq}$, with initial conditions $x(0) = x_0 > 0, y(0) = y_0 > 0$, and $z(0) = z_0 > 0$. Because of the mathematical complexity at the singular point $(0,0,0)$, the ratio-dependent models create richer and more complex dynamics. Next, we follow the idea in [27], that is, since $\lim_{(x,y)} \to (0,0)$, the domain of $\frac{xy}{x+y}$ to $\{(x,y,z)\} : x \geq 0, y \geq 0, z \geq 0$ may be extended so that $(0,0,0)$ becomes a trivial solution to (3). The aim of this study is to examine and illustrate the complexity of the model described above.

3 Preliminaries

In this section, we will discuss the positive invariance and boundedness of solutions for the model (3).

3.1 Positive invariant

As the model in (3) describes prey-predator dynamics, it is crucial to demonstrate the positivity of the solutions. In a biological sense, positivity means that the population remains non-negative (survival of the species). To prove this, we invoke the following theorem from [42].

Theorem 1. All solutions of the model (3) with initial conditions $x_0 > 0$, $y_0 > 0$ and $z_0 > 0$ are positive.

Proof. From (3), we obtained

$$
\begin{aligned}
x(t) &= x_0 \exp\left[\int_0^\tau \left(\left(1-\frac{x}{z}\right)-\frac{a_1 y}{x+y}-h_1\right)dt\right],\\
y(t) &= y_0 \exp\left[\int_0^\tau \left(r_1\left(1-\frac{\gamma y}{z}\right)+\frac{a_2 x}{x+y}-h_2\right)dt\right],\\
z(t) &= z_0 \exp\left[\int_0^\tau (l-mx-ny)\,dt\right].
\end{aligned} \tag{4}
$$

Here, for all $t>0$:

$$\{x_0>0, y_0>0, z_0>0\} \Rightarrow \{x(t)>0, y(t)>0, z(t)>0\},$$

i.e., the positive octant is invariant. □

3.2 Boundedness

Theorem 2. All solutions of model (3) which originates in R^3_+ are uniformly bounded.

Proof. Let us define the function

$$\Omega = a_2x + a_2y + z, \tag{5}$$

which implies that

$$
\begin{aligned}
\frac{d\Omega}{dt} &= a_2x - \frac{a_2x^2}{z} - a_2h_1x + a_1r_1y - \frac{a_1\gamma r_1y^2}{z}\\
&\quad -h_2a_1y + zl - mxz - nyz\\
&= -(a_2x + a_1y + z) + (2a_2 - h_1)x\\
&\quad +(a_1r_1 + a_1 - h_2)y + (1+l)z - \frac{a_2x^2}{z}\\
&\quad -\frac{a_1\gamma r_1y^2}{z} - (mx+ny)z,\\
\frac{d\Omega}{dt}+\Omega &\le \frac{(2a_2-h_1)^2}{4a_2} + \frac{(a_1r_1-h_2)^2}{4a_1\gamma r_1} + \frac{(l+1)^2}{4}\\
&= M,
\end{aligned}
$$

where $M = \frac{(2a_2-h_1)^2}{4a_2} + \frac{(a_1r_1-h_2)^2}{4a_1\gamma r_1} + \frac{(l+1)^2}{4}$.

Integrating the above equation and applying the differential inequality theorem, we have

$$0 < \Omega < M\left(1-e^{-t}\right) + \Omega(x(0), y(0), z(0)),$$

for $t\to\infty$ then we have

$$0 < \Omega < M + \Omega(x(0), y(0), z(0)).$$

Thus, the solution space (x, y, z) is bounded in the region R^3_+. □

4 Existence and Local Stability of Equilibria

In this section, we discuss the existence and local stability of the biologically feasible equilibrium points for the model (3) as follows:

4.1 Existence of Equilibria

For Model (3), we have the following equilibrium points.

1. The trivial equilibrium point $C_0(0,0,0)$ always exists.
2. The prey free equilibrium point $C_1\left(0, \frac{l}{n}, \frac{r_1\gamma l}{(r_1-h_2)n}\right)$.
3. The predator free equilibrium point $C_2\left(\frac{l}{m}, 0, \frac{l}{m(1-h_1)}\right)$.
4. The interior equilibrium point $C^*\left(x^*, y^*, z^*\right)$, where

$$y^* = \frac{l - mx^*}{n},$$
$$z^* = \frac{nr_1 l\gamma x^* + r_1\gamma l^2 + r_1 m^2\gamma x^{*2} - nr_1\gamma m x^{*2} - 2rlmr_1 x^*}{r_1 n^2 x^* + r_1 nl - r_1 nmx^* + a_2 n^2 x^* - h_2 n^2 x^* - lnh_2 + h_2 nmx^*},$$

and x^* is the positive root of the following cubic equation,

$$\sigma_1 x^{*3} + \sigma_2 x^{*2} + \sigma_3 x^* + \sigma_4 = 0, \tag{6}$$

where

$$\begin{aligned}
\sigma_1 =& -mn^2a_2 + n^3a_2 - m^2nh_2 + 2mn^2h_2 \\
& - n^3h_2 + m^2nr_1 - 2mn^2r_1 + n^3r_1 - m^2\gamma r_1 \\
& + 2m^2n\gamma r_1 + m^3\gamma a_1 r_1 - m^2n\gamma a_1 r_1 \\
& + m^3\gamma h_1 r_1 - 2m^2n\gamma h_1 r_1 + mn^2\gamma h_1 r_1, \\
\sigma_2 =& lmnh_2 - ln^2h_2 - lmnr_1 + ln^2r_1 + 3lm^2\gamma r_1 \\
& - 4lmn\gamma r_1 + ln^2\gamma r_1 - 3lm^2\gamma a_1 r_1 \\
& + 2lmn\gamma a_1 r_1 - 3lm^2\gamma h_1 r_1 + 4lmn\gamma h_1 r_1 \\
& - ln^2\gamma h_1 r_1, \\
\sigma_3 =& ln^3a_2 + lmn^2h_2 - ln^3h_2 - lmn^2r_1 + ln^3r_1 \\
& - 3l^3m\gamma r_1 + 3l^2m\gamma a_1 r_1 - l^2n\gamma a_1 r_1 \\
& + 3l^2m\gamma h_1 r_1 - 2l^2n\gamma h_1 r_1, \\
\sigma_4 =& -l^2n^2h_2 + l^2n^2r_1 + l^3\gamma r_1 - l^3\gamma a_1 r_1 - l^3\gamma h_1 r_1.
\end{aligned}$$

It is difficult to say anything about the number of positive roots of Equation (6). We discuss it numerically in the numerical section. Let us assume x^* is the positive root of Equation (6), then $C^*(x^*, y^*, z^*)$ be the interior equilibrium point of the model (3).

Theorem 3. [39] For Model (3), we have

(i). The equilibrium C_1 exists only if $r_1 > h_2$. Similarly, the equilibrium C_2 exists only if $1 > h_1$.

(ii). The interior equilibrium C^* exists, such that x^* is the positive root of Equation (6), and also satisfies $l > mx^*$.

4.2 Local Stability Analysis

First, we consider the conditions for the possibilities of trajectories tending to $(0,0,0)$. For this, we introduce $u = x/y$ and $v = y/z$ and the change of variables $(x,y,z) \to (u,v,z)$. Then, the model (3) can be written as:

$$\begin{aligned}
\frac{du}{dt} &= u\left(1 - uv - \frac{a_1}{u+1} - h_1 - r_1 + r_1\gamma v - \frac{a_2 u}{u+1} + h_2\right),\\
\frac{dv}{dt} &= v\left(r_1 - r_1\gamma v + \frac{a_2 u}{u+1} - h_2 - l + muvz + nvz\right),\\
\frac{dz}{dt} &= z\left(l - muvz - nvz\right),\\
u(0) &> 0, v(0) > 0, z(0) > 0,
\end{aligned} \tag{7}$$

The system (7) has the the equilibrium $C_0(0,0,0)$ and the Jacobian matrix is given by

$$J_{C_0} = \begin{pmatrix} 1 - a_1 - h_1 - h_2 & 0 & 0\\ 0 & r_1 - 2r_1\gamma - h_2 - l & 0\\ 0 & 0 & l \end{pmatrix}. \tag{8}$$

Since one of the eigenvalue, say $\lambda_1 = l > 0$, C_0 is always unstable. A similar analysis can be carried out for other singular points. Further, assume x^* be the positive root of (6) and $C^*(x^*, y^*, z^*)$ be the interior equilibrium point of the model (3). Now, we calculate the Jacobian matrix of the model (3) to analyze the local stability behavior of the model (3) at some arbitrary equilibrium point $C(x,y,z)$, which is given by

$$J(x,y,z) = \begin{pmatrix} P_{11} & P_{12} & P_{13}\\ P_{21} & P_{22} & P_{23}\\ P_{31} & P_{32} & P_{33} \end{pmatrix}, \tag{9}$$

where each entry P_{ij} represents the partial derivative of the corresponding functional response multiplied by its interaction coefficient, ensuring consistency with standard partial derivative notation.

$$\begin{aligned}
P_{11} &= 1 - \frac{2x}{z} - \frac{a_1 y^2}{(x+y)^2} - h_1, \quad P_{12} = -\frac{a_1 x^2}{(x+y)^2},\\
P_{13} &= \frac{x^2}{z^2}, \quad P_{21} = \frac{a_2 y^2}{(x+y)^2},\\
P_{22} &= r_1 - \frac{2r_1\gamma y}{z} + \frac{a_2 x^2}{(x+y)^2} - h_2, P_{23} = \frac{r_1\gamma y^2}{z^2},\\
P_{31} &= -mz, \quad P_{32} = -nz, P_{33} = l - mx - ny.
\end{aligned}$$

Theorem 4. For Model (3),

i. The prey free equilibrium point C_1 is locally asymptotically stable if $1 < a_1 + h_2$.

ii. The predator-free equilibrium point C_2 is locally asymptotically stable, if $h_2 > r_1 + a_2$ and undergoes a transcritical bifurcation if $h_2 = r_1 + a_2$.

Proof. i. The Jacobian matrix at C_1 is given below

$$J_{C_1} = \begin{pmatrix} 1-a_1-h_1 & 0 & 0 \\ a_2 & h_2-r_1 & \frac{(r_1-h_2)^2}{r_1\gamma} \\ \frac{-mr_1\gamma l}{(r_1-h_2)n} & \frac{-r_1\gamma l}{(r_1-h_2)} & 0 \end{pmatrix},$$

the eigenvalues of the Jacobian matrix at C_1 are

$$\lambda_1 = 1-a_1-h_1,$$
$$\lambda_{2,3} = \frac{1}{2}\left((h_2-r_1) \pm \sqrt{(r_1-h_2)^2 - 4(r_1-h_2)l}\right).$$

Hence, C_1 is locally asymptotically stable, if $1 < a_1 + h_2$.

ii. The Jacobian matrix at C_2 is

$$J_{C_2} = \begin{pmatrix} h_1-1 & -a_1 & (1-h_1)^2 \\ 0 & r_1+a_2-h_2 & 0 \\ \frac{-l}{1-h_1} & \frac{-nl}{m(1-h_1)} & 0 \end{pmatrix},$$

the eigenvalues of the Jacobian matrix at C_2 are

$$\lambda_1 = r_1 + a_2 - h_2,$$
$$\lambda_{2,3} = \frac{1}{2}\left((h_1-1) \pm \sqrt{(h_1-1)^2 - 4\,(1-h_1)\,l}\right).$$

Thus, if $h_2 > r_1 + a_2$, then C_2 is locally asymptotically stable. Further, the model undergoes a transcritical bifurcation if

$$h_2 = r_1 + a_2.$$

□

Theorem 5. The interior equilibrium point $C^*(x^*, y^*, z^*)$ locally asymptotically stable if $\frac{a_1xy}{(x+y)^2} - \frac{x}{y} - \frac{r_1\gamma y}{z} - \frac{a_2xy}{(x+y)^2} < 0, a_1 < a_2$ and $2a_1r_1\gamma x^2y^2(x+y)^2 + a_2x^3y^2z > a_1r_1\gamma x^2y^3z$.

Proof. The Jacobian matrix at C^* is given by

$$J_{C^*} = \begin{pmatrix} c_{11} & c_{12} & c_{13} \\ c_{21} & c_{22} & c_{23} \\ c_{31} & c_{32} & 0 \end{pmatrix},$$

and the characteristic equation is

$$\lambda^3 + n_1\lambda^2 + n_2\lambda + n_3 = 0, \tag{10}$$

where

$$n_1 = -c_{11} - c_{22},$$
$$n_2 = c_{11}c_{22} - c_{23}c_{32} - c_{21}c_{12} - c_{13}c_{31},$$

$$
\begin{aligned}
n_3 =& c_{11}c_{22}c_{32} + c_{13}c_{22}c_{31} - c_{12}c_{23}c_{31} - c_{13}c_{21}c_{32},\\
c_{11} =& \frac{a_1x^*y^*}{(x^*+y^*)^2} - \frac{x^*}{z^*},\ c_{12} = \frac{-a_1x^{*2}}{(x^*+y^*)^2},\ c_{13} = \frac{x^{*2}}{z^{*2}},\\
c_{21} =& \frac{a_2y^{*2}}{(x^*+y^*)^2},\ c_{22} = \frac{-r_1\gamma y^*}{z^*} - \frac{a_2x^*y^*}{(x^*+y^*)},\\
c_{23} =& \frac{r_1\gamma y^{*2}}{z^{*2}},\ c_{31} = -mz^*,\ c_{32} = -nz^*.
\end{aligned}
$$

Therefore,

$$
\begin{aligned}
n_1n_2 - n_3 =& (a_2-a_1)\left[\frac{2a_1r_1\gamma x^{*2}y^{*2}}{(x^*+y^*)^2z^{*2}} + \frac{a_2x^{*3}y^{*2}}{(x^*+y^*)^4z^*} - \frac{a_1r_1\gamma x^{*2}y^{*3}}{(x^*+y^*)^4z^*}\right]\\
&+ \frac{3x^{*3}}{z^{*2}} + \frac{r_1\gamma x^{*2}y^*}{z^{*3}} + \frac{mx^{*2}y^*}{(x^*+y^*)^2z^*}(a_1r_1y^* - a_2x^*)\\
&+ \frac{a_2x^{*2}y^*}{(x^*+y^*)^2z^*}\left(\frac{x^*}{z^*} - ny^*\right) + \frac{r_1^2\gamma^2x^*y^{*2}}{(x^*+y^*)^2z^{*2}}.
\end{aligned}
$$

Now, $n_1 > 0, n_3 > 0$ and $n_1n_2 - n_3 > 0$ if

$$
\frac{a_1x^*y^*}{(x^*+y^*)^2} - \frac{x^*}{y^*} - \frac{r_1\gamma y^*}{z^*} - \frac{a_2x^*y^*}{(x^*+y^*)^2} < 0, \quad a_1 < a_2,
$$

and

$$
2a_1r_1\gamma x^{*2}y^{*2}(x^*+y^*)^2 + a_2x^{*3}y^{*2}z^* > a_1r_1\gamma x^{*2}y^{*3}z^*.
$$

Ecologically, This implies that the prey population must grow sufficiently to withstand predation and harvesting, while predator efficiency and resource conversion rates must be high enough relative to predator mortality. Together, these conditions ensure that both prey and predator populations persist at stable levels, avoiding extinction or uncontrolled growth. Therefore, by Routh-Hurwitz criteria [31], the interior equilibrium point $C^*(x^*, y^*, z^*)$ is locally asymptotically stable. □

5 Bifurcation Analysis

In this section, we analyze the bifurcation of the model (3) analytically, according to the harvesting effect.

5.1 Hopf-Bifurcation

The local birth or death of a periodic solution around the equilibrium is known to be a Hopf bifurcation. The following theorem provides the condition for the existence of Hopf-bifurcation with respect to the harvesting parameter as a bifurcation parameter.

Theorem 6. The model (3) is subject to a Hopf-bifurcation if the bifurcation parameter h^* (as a harvest parameter) exceeds a critical value. The condition for the occurrence of the Hopf-bifurcation at $h = h^*$ is as follows

1. $n_1(h^*)n_2(h^*) - n_3(h^*) = 0$,

2. $\frac{d}{dh^*}(Re(\lambda(h^*)))\big|_{h=h^*} \neq 0$,
   where λ is the root of the characteristic equation associated with interior equilibrium point E^*.

Proof. For $h = h^*$, let the characteristic Equation (10) is in the form of

$$\left(\lambda^2(h^*) + n_2(h^*)\right)\right)\left(\lambda(h^*) + n_1(h^*)\right) = 0. \tag{11}$$

Thus, $\pm i\sqrt{n_2(h^*)}$ and $-n_1(h^*)$ are the roots of (11). For the occurrence of the Hopf-bifurcation, at $h_1 = h^*$, it must meet the following transversality condition

$$\frac{d}{dh^*}(Re(\lambda(h^*)))\Big|_{h=h^*} \neq 0.$$

For all h, the roots are generally in the form

$$\lambda_{1,2}(h) = e(h) \pm if(h),$$
$$\lambda_3(h) = -n_2(h).$$

Substituting, $\lambda_{1,2}(h) = e(h) + if(h)$ in (11), we have

$$M(h) + iN(h) = 0,$$

where

$$\begin{aligned} M(h) =& e^3(h) + e^2(h)n_1(h) - 3e(h)f^2(h) \\ & - f^2(h)n_1(h) + n_2(h)e(h) + n_1(h)n_2(h), \\ N(h) =& n_2(h)f(h) + 2e(h)f(h)n_1(h) \\ & + 3e^2(h)f(h) - f^3(h). \end{aligned}$$

To accomplish Equation (11), we should have $M(h) = 0$ and $N(h) = 0$, then differentiate M and N with respect to h, we get

$$\frac{dM}{dh} = \rho_1(h)e'(h) - \rho_2 f'(h) + \rho_3(h) = 0, \tag{12}$$
$$\frac{dN}{dh} = \rho_2(h)e'(h) + \rho_1(h)f'(h) + \rho_4(h) = 0, \tag{13}$$

where

$$\begin{aligned} \rho_1(h) =& 3e^2(h) + 2e(h)n_1(h) - 2f'(h) + n_2(h), \\ \rho_2(h) =& 6e(h)f(h) + 2f(h)n_1(h), \\ \rho_3(h) =& e^2(h)n_1'(h) - f^2(h)n_1'(h) + n_2'(h)e(h), \\ \rho_4(h) =& 2e(h)f(h)n_1'(h) + n_2'(h)f(h). \end{aligned}$$

On multiply, (12) and (13) by $\rho_1(h)$ and $\rho_2(h)$ respectively, then add those equations, we get

$$e'(h) = -\frac{\rho_1(h)\rho_3(h) + \rho_2(h)\rho_4(h)}{\rho_1^2(h) + \rho_2^2(h)}, \tag{14}$$

substituting, $\rho_1(h) = 0$ and $f(h) = \sqrt{n_2(h)}$ on $\rho_1(h), \rho_2(h), \rho_3(h)$ and $\rho(h)$at $h = h^*$, we obtain

$$\begin{aligned}
&\rho_1(h^*) = -2n_2(h^*), \rho_2(h^*) = 2n_1(h^*)\sqrt{n_2(h^*)},\\
&\rho_2(h^*) = n_3'(h^*) - n_2(h^*)n_1'(h^*),\\
&\rho_4(h^*) = n_2'(h^*)\sqrt{n_2(h^*)}.
\end{aligned}$$

Equation (14) implies

$$e'(h^*) = \frac{n_3'(h^*) - (n_1(h^*)n_2(h^*))'}{2(n_2^2(h^*) + n_1^2(h^*))}.$$

If $n_3'(h^*) - (n_1(h^*)n_2(h^*))' \neq 0$, which implies that $\frac{d}{dh^*}(Re(\lambda(h^*)))\big|_{h=h^*} \neq 0, j = 1, 2$. This indicates that oscillatory dynamics (population cycles) emerge when the interaction strengths and growth rates cross a critical threshold. For example, if predation efficiency or harvesting rate exceeds certain values, the system shifts from stable coexistence to sustained oscillations.Hence, the above condition is guaranteed the transversality condition, i.e., the model (3) exhibits the Hopf-bifurcation at $h = h^*$. The numerically determined critical value h_2^* confirms the predicted Hopf bifurcation condition in this Theorem, showing how the loss of equilibrium stability depends on the harvesting parameter. □

5.2 Transcritical Bifurcation

In the following theorems, the existence of transcritical bifurcation has been established using Sotomayor's theorem [39] about the two equilibrium points $C_2(\frac{l}{m}, 0, \frac{l}{m(1-h_1)})$ and $C^*(x^*, y^*, z^*)$.

Theorem 7. The model (3) undergoes a transcritical bifurcation about $C_2(\frac{l}{m}, 0, \frac{l}{m(1-h_1)})$ as the parameter h_2 crosses the critical value $h_2^* = r_1 + a_2$.

Proof. Let $X = (x, y, z)$ and

$$f(X, h_2) = \begin{pmatrix} x\left(1 - \frac{x}{z}\right) - \frac{a_1 xy}{x+y} - h_1 x \\ r_1 y\left(1 - \frac{\gamma y}{z}\right) + \frac{a_2 xy}{x+y} - h_2 y \\ z\left(l - mx - ny\right) \end{pmatrix},$$

$$f_{h_2}(C_2, h_2) = \begin{pmatrix} 0 \\ 0 \\ 0 \end{pmatrix},$$

$$Df_{h_2}(X, h_2) = \begin{pmatrix} 0 & 0 & 0 \\ 0 & -1 & 0 \\ 0 & 0 & 0 \end{pmatrix},$$

$$A = Df(C_2, h_2^*) := \begin{pmatrix} -1+h_1 & -a_1 & (1-h_1)^2 \\ 0 & 0 & 0 \\ \frac{-l}{1-h_1} & \frac{-ln}{m(1-h_1)} & 0 \end{pmatrix}.$$

Let $V = (v_1, v_2, v_3)^T$ with $v_1 = \frac{-ln}{m}$, $v_2 = 1$, and $v_3 = \frac{a_1 m - ln(1-h_1)}{m(1-h_1)^2}$ and $W = (0,1,1)^T$, be the eigenvectors of A and A^T, respectively corresponding to zero eigenvalue. Now, the three conditions of Sotomayor's theorem are computed below:

(i) $W^T f_{h_2}(C_2, h_2^*) = 0$,

(ii) $W^T[Df_{h_2}(C_2, h_2^*)V] = \begin{pmatrix} 0 & 1 & 1 \end{pmatrix} \left[\begin{pmatrix} 0 & 0 & 0 \\ 0 & -1 & 0 \\ 0 & 0 & 0 \end{pmatrix} \begin{pmatrix} v_1 \\ 1 \\ v_3 \end{pmatrix} \right] = -1 \neq 0$

(iii) $W^T[D^2 f(C_2, h_2^*)(V,V)] = -2nv_3 - \frac{2a_2 m}{l} - \frac{2r_1\gamma m(1-h_1)}{l} \neq 0.$

By Sotomayor Theorem [39], Model (3) undergoes a transcritical bifurcation at the equilibrium point C_2 as the parameter h_2 varies through the bifurcation value $h_2 = h_2^*$. □

Theorem 8. Model (3) undergoes a transcritical bifurcation about $C^*(x^*, y^* z^*)$ as the parameter h_2 crosses the critical value $h_2^* = r_1 + a_2$.

Proof. Let X and $f(X, h_2)$ are same as in Theorem 7.

$$f_{h_2}(C^*, h_2) = \begin{pmatrix} 0 \\ -y^* \\ 0 \end{pmatrix},$$

$$Df_{h_2}(X, h_2) = \begin{pmatrix} 0 & 0 & 0 \\ 0 & -1 & 0 \\ 0 & 0 & 0 \end{pmatrix},$$

$$\begin{aligned} B &= Df(C^*, h_2^*) \\ &= \begin{pmatrix} \frac{a_1 x^* y^*}{(x^*+y^*)^2} - \frac{x^*}{z^*} & \frac{-a_1 x^{*2}}{(x^*+y^*)^2} & \frac{x^{*2}}{z^{*2}} \\ \frac{a_2 y^{*2}}{(x^*+y^*)^2} & \frac{-r_1\gamma y^*}{z^*} - \frac{a_2 x^* y^*}{(x^*+y^*)} & \frac{r_1\gamma y^{*2}}{z^{*2}} \\ -mz^* & -nz^* & 0 \end{pmatrix}. \end{aligned}$$

Let $\bar{V} = (\bar{v_1}, \bar{v_2}, \bar{v_3})^T$ and $\bar{W} = (\bar{w_1}, \bar{w_2}, \bar{w_3})^T$, be the eigenvectors of B and B^T, respectively corresponding to zero eigenvalue. Now the three conditions of Sotomayor's theorem are computed below:

(i) $\bar{W}^T f_{h_2}(C^*, h_2^*) = 0$,

(ii) $\bar{W}^T[Df_{h_2}(C^*, h_2^*)\bar{V}] \neq 0$

(iii) $\bar{W}^T[D^2 f(C^*, h_2^*)(\bar{V}, \bar{V})] \neq 0.$

We see that $h_2 = r_1 + a_2$, the equilibrium C^* becomes C_2. Then the values of is (i), (ii), and (iii) are similar to the Theorem 7. By Sotomayor Theorem [39], the model (3) undergoes a transcritical bifurcation at the equilibrium point C^* as the parameter h_2 varies through the bifurcation value $h_2 = h_2^*$. □

6 Bionomic Equilibrium and Optimal Harvesting

6.1 Bionomic Equilibrium

The term bionomic equilibrium is a combination of the concepts of biological equilibrium and economic equilibrium [22]. From the model (2), a biological equilibrium is provided by

$$\frac{dX}{dt} = \frac{dY}{dt} = \frac{dZ}{dt} = 0.$$

Let s_1, s_2 be the cost of harvesting per unit effort of intraguild prey and intraguild predator, respectively, and $p_1 p_2$ be the price per unit biomass of the intraguild prey and intraguild predator. Then, the economic rent at any time is given by

$$\begin{aligned}\pi =&(p_1 x - s_1)E_1 + (p_2 y - s_2)E_2\\ =&\pi_1 + \pi_2.\end{aligned}$$

Here, π_1 and π_2 are the net revenues of intraguild prey and intraguild predator species, respectively. Bionomic equilibrium $(x_\infty, y_\infty, z_\infty, E_{1\infty}, E_{2\infty})$ is obtained by solving the following simultaneous equations. (The X, Y, Z variables are uppercase in the model (2), now which are considered lowercase in this section):

$$c_1\left(1 - \frac{x}{pz}\right) - \frac{\alpha y}{x + ay} - E_1 = 0, \tag{15}$$

$$c_2\left(1 - \frac{y}{qz}\right) + \frac{\beta x}{x + ay} - E_2 = 0, \tag{16}$$

$$(c - ux - vy) = 0, \tag{17}$$

$$\pi = (p_1 x - s_1)E_1 + (p_2 y - s_2)E_2 = 0. \tag{18}$$

To determine the bioeconomic equilibrium, we now consider the following cases.

- **Case I:** If $s_1 > p_1 x$, then the cost is greater than the revenue for intraguild prey species, the intraguild prey harvesting will be closed i.e., $E_1 = 0$. Only intraguild predator harvesting will be operational.
  From (15)-(17), we have

$$y_\infty = \frac{s_2}{p_2}, \tag{19}$$

$$x_\infty = \frac{cp_2 - vs_2}{p_2 u}, \tag{20}$$

$$z_\infty = \frac{c_1\left(cp_2 - vs_2\right)\left(\left(cp_2 - vs_2\right) + aus_2\right)}{pup_2\left(\left(c_1\left(cp_2 - vs_2\right) + aus_2\right) - \alpha us_2\right)}. \tag{21}$$

  Using (19)-(21) in (15) we obtain

$$\begin{aligned}E_{2\infty} =&\frac{c_1 c_2 q\left(cp_2 - vs_2\right)\left(\left(cp_2 - vs_2\right) + auc_2\right)}{qc_1\left(cp_2 - vs_2\right)\left(cp_2 - vs_2 + aus_2\right)}\\ &-\frac{c_2 s_2 pu\left(\left(c_1\left(cp_2 - vs_2\right) + aus_2\right) - \alpha us_2\right)}{qc_1\left(cp_2 - vs_2\right)\left(cp_2 - vs_2 + aus_2\right)}\end{aligned}$$

$$+\frac{\beta q c_1(cp_2-vs_2)}{qc_1\left(cp_2-vs_2\right)\left(cp_2-vs_2+aus_2\right)}. \tag{22}$$

Therefore, $E_{2\infty}>0$, if

$$\begin{aligned} &c_1c_2q(cp_2-vs_2)\left((cp_2-vs_2)+auc_2\right)+\beta qc_1(cp_2-vs_2)\\ &>c_2s_2pu\left(\left(c_1\left(cp_2-vs_2\right)+aus_2\right)+\alpha us_2\right)\end{aligned}$$

- **Case II:** If $s_2>p_2y$, that is, the cost exceeds the revenue for the intraguild predator, the intraguild predator harvesting will be discontinued, i.e., $E_2=0$. Only intraguild prey harvesting remains active. Again, from Equations (15)-(17), we derive:

$$y_\infty=\frac{s_1}{p_1}, \tag{23}$$

$$x_\infty=\frac{cp_1-us_1}{p_1v}, \tag{24}$$

$$z_\infty=\frac{\left(cp_1-us_1\right)\left(c_2s_1v+c_2a\left(cp_1-us_1\right)\right)}{qvp_1\left(c_2s_1v+c_2a\left(cp_1-us_1\right)+\beta vs_1\right)}. \tag{25}$$

Using (23)-(25) in (15), we obtain

$$\begin{aligned} E_{1\infty}=&\frac{c_1p(cp_1-us_1)(s_1v+a\left(cp_1-us_1\right))}{pc_2\left(cp_1-us_1\right)\left(s_1v+a\left(cp_1-us_1\right)\right)}\\ &-\frac{c_1s_1qv(c_2s_1v+c_2a(cp_1-us_1)+\beta vs_1)}{pc_2\left(cp_1-us_1\right)\left(s_1v+a\left(cp_1-us_1\right)\right)}\\ &-\frac{\alpha pc_2(cp_1-us_1)}{pc_2\left(cp_1-us_1\right)\left(s_1v+a\left(cp_1-us_1\right)\right)}.\end{aligned} \tag{26}$$

Therefore, $E_{1\infty}>0$, if

$$\begin{aligned} c_1p(cp_1-us_1)(s_1v+a\left(cp_1-us_1\right))>&\ \alpha pc_2(cp_1-us_1)\\ &+c_1s_1qv(c_2s_1v+c_2a(cp_1-us_1)+\beta vs_1)\,.\end{aligned}$$

- **Case III:** If $s_1<p_1x$ and $s_2<p_2y$, then the whole model will be in operation, and it gives

$$\begin{aligned} x_\infty&=\frac{s_1}{p_1},\\ y_\infty&=\frac{s_2}{p_2}.\end{aligned}$$

Here, the biological parameters c,u,v and the economical parameters c_1,c_2,p_1,p_2 must satisfy the relation

$$c=\frac{us_1p_1+vs_2p_2}{p_1p_2}.$$

From (15), we have

$$z\left[E_1+\frac{\alpha s_2p_1}{s_1p_2+ap_1s_2}-c_1\right]+\frac{c_1s_1}{pp_1}=0. \tag{27}$$

Similarly, from (16), we obtain

$$z\left[E_2-\frac{\beta s_1p_2}{s_1p_2+ap_1s_2}-c_2\right]+\frac{c_2s_2}{qp_2}=0. \tag{28}$$

6.2 Optimal Harvesting Policy

We formulate the optimal harvesting problem for the nondimensionalized system, aiming to maximize the discounted net revenue from harvesting both the prey and the intermediate predator.

$$J(E_1, E_2) = \int_0^\infty e^{-\delta t}((p_1 x - s_1)E_1 + (p_2 y - s_2)E_2)\, dt, \tag{29}$$

where $x(t)$ and $y(t)$ are prey and intermediate predator densities, $E_1(t)$ and $E_2(t)$ are harvesting efforts, p_1, p_2 are unit prices, s_1, s_2 are harvesting costs, and $\delta > 0$ is the discount rate.

Subject to the constraints of (2) is

$$0 \le E_i(t) \le E_i^{\max}, \quad i = 1, 2. \tag{30}$$

By *Pontryagin's maximum principle*, we construct the Hamiltonian as follows for this problem:

$$\begin{aligned} H =& e^{-\delta t}\left((p_1 x - s_1)E_1 + (p_2 y - s_2)E_2\right) \\ &+ \lambda_1 \left(c_1 x \left(1 - \frac{x}{pz}\right) - \frac{\alpha x y}{x + a y} - E_1 x\right) \\ &+ \lambda_2 \left(c_2 y \left(1 - \frac{y}{qz}\right) + \frac{\beta x y}{x + a y} - E_2 y\right) \\ &+ \lambda_3 \left(z(c - ux - vy)\right), \end{aligned}$$

where, the adjoint variable are $\lambda_i = \lambda_i(t), \quad i = 1, 2, 3.$
Now, $\frac{\partial H}{\partial E_1} = 0$, $\frac{\partial H}{\partial E_2} = 0$, we have

$$\lambda_1 = e^{-\delta t}\left(p_1 - \frac{s_1}{x}\right), \tag{31}$$

$$\lambda_2 = e^{-\delta t}\left(p_2 - \frac{s_2}{y}\right). \tag{32}$$

Then, adjoint equations are

$$\frac{d\lambda_1}{dt} = -\frac{\partial H}{\partial x}, \frac{d\lambda_2}{dt} = -\frac{\partial H}{\partial y}, \frac{d\lambda_3}{dt} = -\frac{\partial H}{\partial z}. \tag{33}$$

Using H and the third equation of (33), we obtain

$$\frac{d\lambda_3}{dt} = -\frac{\partial H}{\partial x} = -\left(\lambda_1 \frac{c_1 x^2}{pz^2} + \lambda_2 \frac{c_2 y^2}{qz^2} + \lambda_3(c - ux - vy)\right),$$

which implies

$$\frac{d\lambda_3}{dt} = -\lambda_1 \frac{c_1 x^2}{pz^2} - \lambda_2 \frac{c_2 y^2}{qz^2}.$$

From (31) and (32), we get

$$\frac{d\lambda_3}{dt} = -e^{-\delta t}\left(p_1 - \frac{s_1}{x}\right)\frac{c_1 x^2}{pz^2} - e^{-\delta t}\left(p_2 - \frac{s_2}{y}\right)\frac{c_2 y^2}{qz^2},$$

which implies

$$\lambda_3 = \frac{e^{-\delta t}}{\delta}\left[\left(p_1 - \frac{s_1}{x}\right)\frac{c_1 x^2}{pz^2} + \left(p_2 - \frac{s_2}{y}\right)\frac{c_2 y^2}{qz^2}\right]. \tag{34}$$

Let, the constant of integration vanishes, hence $\lambda_i e^{\delta t}(i = 1, 2, 3)$ of three species are bounded. Using (31) and (32), we get from the first two adjoint equations in (33)

$$\delta e^{-\delta t}\left(p_1 - \frac{s_1}{x}\right) = -\left(e^{-\delta t}p_1 E_1 + \lambda_1\left(\frac{\alpha xy}{(x+ay)^2} - \frac{c_1 x}{pz}\right) + \lambda_2 \frac{a\beta y^2}{(x+ay)^2} - \lambda_3 uz\right), \tag{35}$$

and

$$\delta e^{-\delta t}\left(p_2 - \frac{s_2}{y}\right) = -\left(e^{-\delta t}p_2 E_2 + \lambda_1 \frac{\alpha x^2}{(x+ay)^2} - \lambda_2\left(\frac{a\beta xy}{(x+ay)^2} + \frac{c_2 y}{qz}\right) - \lambda_3 vz\right). \tag{36}$$

Applying the equilibrium condition and substituting values of λ_i, for $i = 1, 2, 3$ in (35) and (36), we get

$$\begin{aligned} p_1 E_1 =& \delta\left(p_1 - \frac{s_1}{x}\right) + \left(p_1 - \frac{s_1}{x}\right)\left(\frac{\alpha xy}{(x+ay)^2} - \frac{c_1 x}{pz}\right) \\ &+ \left(p_2 - \frac{s_2}{y}\right)\frac{a\beta y^2}{(x+ay)^2} \\ &- \frac{u}{\delta z}\left(\frac{c_1 x^2}{p}\left(p_1 - \frac{s_1}{x}\right) + \frac{c_2 y^2}{q}\left(p_2 - \frac{s_2}{y}\right)\right), \end{aligned}$$

and

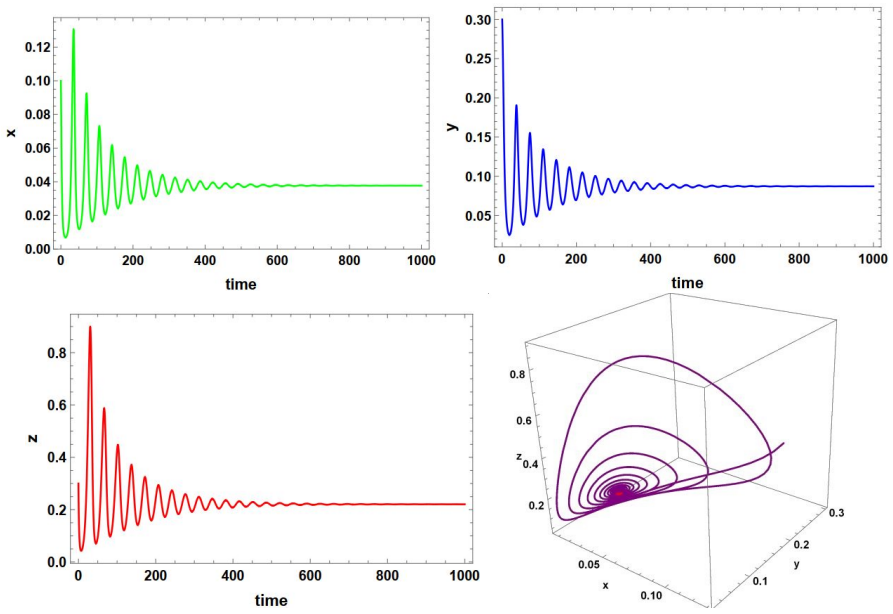

Figure 2: The locally asymptotically stable time series (a), (b), (c) and phase portrait (d) for the model (3) parameters values in (39) with $h_1 = 0.48$ and $h_2 = 0.25$ near $C^*(0.037733, 0.0871706, 0.220599)$.

$$p_2 E_2 = \delta\left(p_2 - \frac{s_2}{y}\right) + \left(p_1 - \frac{s_1}{x}\right)\left(\frac{\alpha x^2}{(x+ay)^2}\right)$$

$$- \left(p_2 - \frac{s_2}{y}\right)\left(\frac{a\beta xy}{(x+ay)^2} - \frac{c_2 y}{qz}\right)$$
$$- \frac{v}{\delta z}\left(\frac{c_1 x^2}{p}\left(p_1 - \frac{s_1}{x}\right) + \frac{c_2 y^2}{q}\left(p_2 - \frac{s_2}{y}\right)\right).$$

The above equations provide the optimal harvesting efforts as follows:

$$E_1 = \frac{1}{p_1}\left(p_1 - \frac{s_1}{x}\right)\left(\delta + \frac{\alpha xy}{(x+ay)^2} - \frac{c_1 x}{pz} - \frac{uc_1 x^2}{\delta pz}\right)$$
$$+ \frac{1}{p_1}\left(p_2 - \frac{s_2}{y}\right)\left(\frac{a\beta y^2}{(x+ay)^2} - \frac{uc_2 y^2}{\delta qz}\right), \tag{37}$$

and

$$E_2 = \frac{1}{p_2}\left(\left(p_1 - \frac{s_1}{x}\right)\left(\frac{\alpha x^2}{(x+ay)^2} - \frac{vc_1 x^2}{p\delta z}\right)\right.$$
$$\left. + \left(p_2 - \frac{s_2}{y}\right)\left(\delta - \left(\frac{a\beta xy}{(x+ay)^2} + \frac{c_2 xy}{qz}\right) - \frac{vc_2 y^2}{\delta qz}\right)\right). \tag{38}$$

Hence, solve the (37) and (38) together with steady-state equations we get an optimal solutions $(x_\delta,\ y_\delta,\ z_\delta)$ and the optimal harvesting efforts E_1 and E_2.

7 Numerical Results

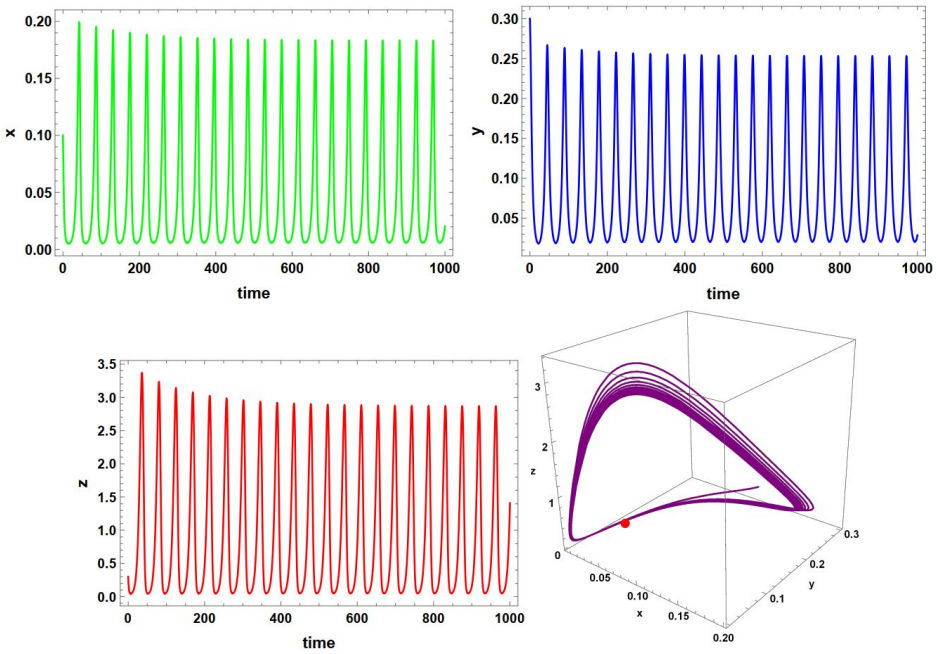

Figure 3: The occurrence of periodic solution in time series (a), (b), (c) and phase portrait (d) for the model (3) with the parameter values in (39), $h_1 = 0.53$, and $h_2 = 0.25$ near $C^*(0.0372941, 0.0873199, 0.3117236)$.

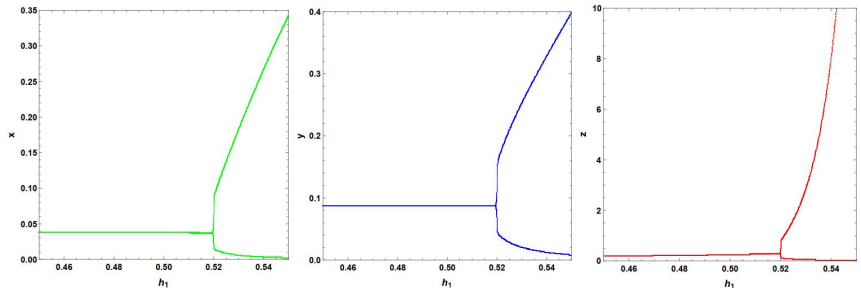

Figure 4: The bifurcation diagrams for the model (3) with parameter values in (39), $h_2 = 0.25$, and $h_1 \in (0.1, 0.6)$.

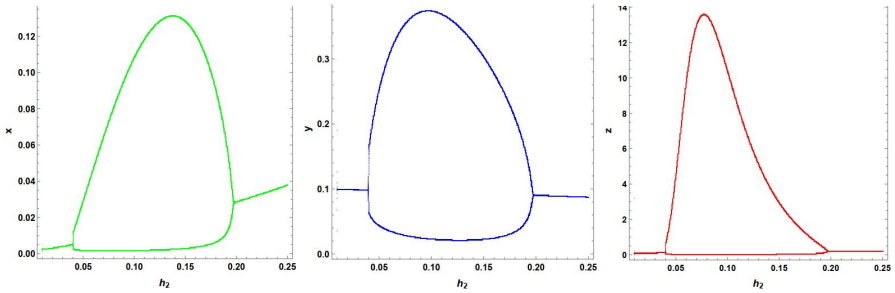

Figure 5: The bifurcation diagrams for (3) with parameter values in (39), $h_1 = 0.48$, and $h_2 \in (0.01, 0.25)$.

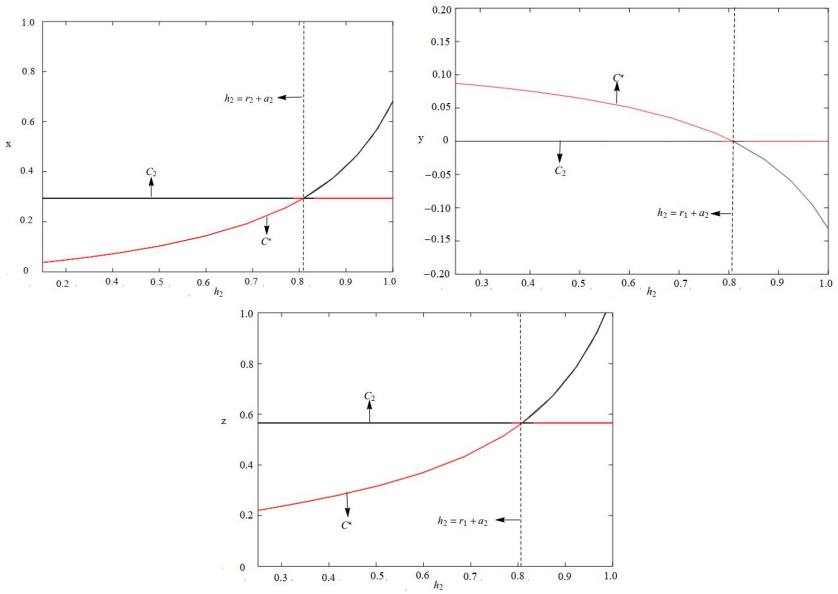

Figure 6: The x, y, and z components of equilibria C_2 and C^* for (3) with parameter values in (39), $h_1 = 0.48$ and $h_2 \in (0.1, 1)$. The red curves represent the stable and black curves represent the unstable branches of the equilibria C_2 and C^*, respectively. The Hopf bifurcation occurs at h_2^*, marked by the vertical dashed line, indicating the transition from stable equilibrium to periodic oscillations.

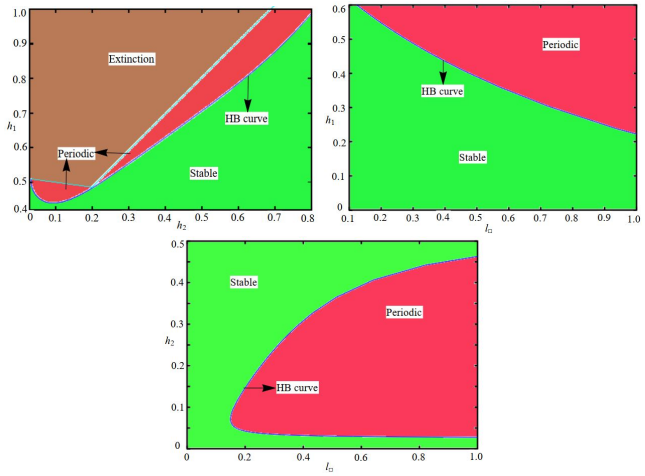

Figure 7: The two-parameter bifurcation diagram for the model (3) in (a) $h_2 \in (0.01, 0.8)$ vs $h_1 \in (0.4, 1.0)$, (b) $l \in (0.1, 1.0)$ vs $h_1 \in (0, 0.6)$, and (c) $l \in (0, 1)$ vs $h_2 \in (0, 0.5)$ with other parameters are given in (39). The blue color line denotes the Hopf bifurcation (HB) curve, which separates the stable and periodic regions. The cyan color line separates the periodic and population extinction regions. The stable region is denoted in green, the periodic region is given in red, and the brown color represents the region where the populations become extinct.

In order to verify the analytical findings and stability results obtained in the previous sections, we numerically simulate the solutions of the model (3). We perform numerical tests for the model (3) with a different set of parameter values. Now, we consider the set of values of the parameters as

$$\begin{aligned} a_1 = 0.50, r_1 = 0.019, a_2 = 0.79, \gamma = 1.02, \\ l = 0.25, m = 0.85, \text{ and } n = 2.5. \end{aligned} \tag{39}$$

The parameter r_1 is the intrinsic (per-capita) growth rate of prey species, expressed per unit time. By contrast, a_2 is an attack/interaction coefficient (rate of successful encounters per predator per prey) and has a different dimensional interpretation. Parameters of different types are not expected to have similar numerical magnitudes because they measure different processes and have different units. If the time unit in the model is years, $r_1 = 0.019$ corresponds to a per-year growth rate of 1.9% which is entirely plausible for long-lived species or populations under strong resource limitation or exploitation. If the time unit is days, the value likewise represents a very slow-growing population (≈1.9% per day integrated rate), which may be appropriate for certain biological or managed populations. We now state the model's time units explicitly and note that an intrinsic growth rate of this order is consistent with species that reproduce slowly or have strong density dependence/harvesting pressure.

Now, we investigate the harvesting parameters individually. In order to show the effect of harvesting parameters in the considered model. Assume $h_1 = 0.48$ and $h_2 = 0.25$, and the model (3) is locally asymptotically stable about the interior equilibrium point $C^*(0.037733, 0.0871706, 0.220599)$, with the remaining parameter values in (39), as shown in the time series and phase portrait in Figure 3 The stable behavior indicates that the small fluctuations in initial population size do not affect the population over a longer period of time, i.e., the long-term survival of both species. When we increase the value of h_1 at some critical value, $h_1 = 0.51895$, the model (3) loses its stability and undergoes Hopf bifurcation. Also, satisfy the Theorem 6, i.e., $n_1(h_1^*)n_2(h_1^*) - n_3(h_1^*) = 0$ and $n_3'(h_1^*) - (n_1(h_1^*)n_2(h_1^*))' = -0.024916 \neq$

0 which ensure the existence of Hopf bifurcation. The existence of a periodic solution in time serious and phase portrait for the model (3) at $h_1 = 0.53$ near $C^*(0.0372941, 0.0873199, 0.3117236)$ is shown in Figure 3. For clear representation, the one-parameter bifurcation diagram with parameters in (39), $h_2 = 0.25$, and $h_1 \in (0.45, 0.55)$ is plotted in the Figure 4.

It is also necessary to investigate the impact of another harvesting parameter h_2. To validate the bifurcation structure, we performed eigenvalue continuation and time-series simulations from multiple initial conditions. The results show coexistence of a stable equilibrium and a stable limit cycle for certain values of h_2, confirming bistability. This indicates a subcritical Hopf bifurcation followed by a fold of limit cycles. Accordingly, Figure 5 has been updated to display both the stable equilibrium branch and the stable periodic orbit branch. For a detailed understanding of the dynamics. We chose the parameter values in (39), $h_1 = 0.48$ and vary $h_2 \in (0.01, 0.25)$, and plotted the one-parameter bifurcation diagram in Figure 5. It shows that the model (3) is locally asymptotically stable for $h_2 \in (0, 0.04)$, periodic solution for $h_2 \in (0.04, 0.195)$, and again become locally asymptotically stable near for $h_2 \in (0.195, 0.25)$ near C^*. It is clear that the model (3) undergoes Hopf bifurcation at two points within the parameter range $h_2 \in (0, 0.25)$. On further increasing the value h_2 in the range $h_2 \in (0.25, 1)$, the model (3) exhibits transcritical bifurcation behavior between the equilibrium points C_2 and C^*. First, the equilibrium C^* is stable, whereas C_2 is unstable as h_2 increases and crosses the critical value $h_2 = r_1 + a_2$, then the equilibrium C^* becomes unstable, and C_2 becomes stable, which is depicted in Figure 6. Also, the model (3) satisfy the Theorems 7 and 8 at $h_2 = h_2^* = r_1 + a_2$, which ensures the existence of transcritical bifurcation between C_2 and C^*. When $h_2 = r_1 + a_2$ the model equilibrium C^* becomes C_2, which shows that a higher harvesting rate h_2 in the second species causes to die out y and results in the survival of only species x and z respectively. For a clear illustration, the dynamical changes of the model (3) with the influence of harvesting effects, the two-parameter bifurcation diagrams are plotted in Figure 7. In Figure 7(a) the two-parameter bifurcation diagram is plotted for h_2 and h_1, similarly for l and h_1 in Figure 7(b) and l and h_2 in Figure 7(c). In which the green color represents the stable region, the red color represents the unstable region, and the brown color represents the extinction region. Furthermore, it is helpful to find extinction and survival regions of species with the choice of harvesting parameters h_1 and h_2. Moreover, the nonzero bionomic equilibrium is found on the surface encompassing the two curves, which is illustrated in Figure 8.

Here, we solve the model (2), we obtain the optimal solutions

$$(0.762046195, 0.476130367, 1.928739577)$$

with corresponding optimal efforts are $E_1 = 0.572646$ and $E_2 = 0.809736$. Taking

$$\begin{aligned} &a = 1.5, \quad \alpha = 0.1, \quad \beta = 1.5, \quad c = 1.6, \quad u = 0.85, \quad v = 2, \quad c_1 = p = 1, \\ &c_2 = 0.2, \quad q = 0.3, \quad p_1 = 15, \quad s_1 = 10, \quad p_2 = 25, \quad s_2 = 10 \text{ and } \delta = 5. \end{aligned}$$

Then, we get the maximum value of the net revenues

$$J = \int_0^\infty e^{-5t} 2.52718923 dt = 0.505437846.$$

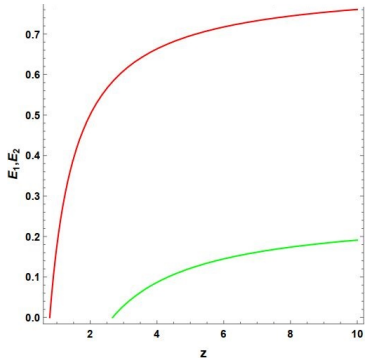

Figure 8: For the set parameters $c_1 = 0.47$, $c_2 = 0.5$, $p_1 = 0.6$, $p_2 = 0.7$, $p = 0.45$, $q = 0.55$ $\alpha = 0.3$, $\beta = 0.5$, $s_1 = 0.4$, $s_2 = 0.5$, $a = 0.5$ red curve indicates z vs. E_2 and green curve indicates z vs. E_1

8 Conclusion

This study examines the population model of the three species, which are intraguild prey, intraguild predators, and biotic resources. The process of population reduction by harvesting takes place in the population. Changes in harvesting parameters in each population provide an understanding of the dynamics of harvesting in the considered model. Bifurcation and stability analysis help us determine the Hopf-bifurcation in our model due to the change in the signs of the associated eigenvalues of the corresponding model. Prey decline in our model is primarily influenced by predation, but because the variable Z affects both prey and predator, extinction arises from their coupled dynamics rather than predation alone. Thus, the mechanism of extinction depends on the parameter regime, with predation dominating in some cases and resource effects amplifying it in others. The coexistence of prey, predator, and biotic resource can exist only in a small parameter range, which is determined by the exact combination of prey and predator assault rates on the resource, as well as the predator's predation rate. We begin by non-dimensionalizing the basic model and reducing the number of parameters. However, the original model has been considered while dealing with the harvesting attempts of E_1 and E_2. These results show that the harvest affects the survival of one or more species in the ecosystem. In our model, we showed how the harvesting parameters help have a greater impact on the survival of species by plotting various bifurcation diagrams. Also, we described the existence of transcritical bifurcation in our considered model, which is a danger sign for species extinction due to over-harvesting. Therefore, we must control harvesting activities to stop population extinction in the ecosystem. Here, we investigated the dynamics of the bionomic equilibrium. Finally, the optimal harvesting policy is derived using Pontryagin's maximum principle. With the control of harvesting efforts, $0 \leq E_i \leq E_i^{max}$ has a definite condition, i.e., the internal equilibrium point is constant and gives maximum profit. Predators and prey populations can coexist, although both populations are harvested by a sustained effort. Using Pontryagin's maximization policy, we found a certain value in the harvest effort, E_1 and E_2, which is related to a fixed equilibrium point that increases the net current revenue.

In this paper, we investigated the intraguild predation model with individual harvesting techniques and ratio-dependent functional responses. As far as future research goes, there are several possibilities

for this study. One important direction is that we can expand on the notion of this article by putting a gestation time delay on the intraguild predator in our examined model. We leave it for future work.

Declarations

Availability of Supporting Data

All data generated or analyzed during this study are included in this published paper.

Funding

The authors conducted this research without any funding, grants, or support.

Conflict of Interest

The authors declare that they have no known competing financial interests or personal relationships that could have influenced the work reported in this paper.

Author Contributions

Subramani Magudeeswaran: Conceptualization, Methodology, Methematical Modeling, Writing - Oringinal Draft. Muthuradhinam Sivabalan: Overall Guidance, Final approval of the manuscript. Mehmet Yavuz: Resources, Validation, Supervision, Project administration. Dharmendra Kumar Singh: Formal analysis, Investigation, Writing - review and editing. Kannimuthu Giridharan: Software, Data curation, validation and visualization. All authors have read and approved the final version of the manuscript.

Artificial Intelligence Statement

Artificial intelligence (AI) tools, including large language models, were used solely for language editing and improving readability. AI tools were not used for generating ideas, performing analyses, interpreting results, or writing the scientific content. All scientific conclusions and intellectual contributions were made exclusively by the authors.

Publisher's Note

The publisher remains neutral regarding jurisdictional claims in published maps and institutional affiliations.

References

[1] Abdullah, S.N., Safuan, H.M., Nor, M.E., Jamaian, S.S., Aman, F., Shab, N.F.M. (2018). "Harvesting effects on population model of competitive interaction with shared biotic resource". *25th National Symposium on Mathematical Sciences (SKSM25): Mathematical Sciences as the Core of Intellectual Excellence, Malaysia*, 1974(1), doi:https://doi.org/10.1063/1.5041609.

[2] Abou-nouh, H., El Khomssi, M. (2025). "Towards a viable control strategy for a model describing the dynamics of corruption". *Mathematical Modelling and Numerical Simulation with Applications*, 5(1), 1-17, doi:https://doi.org/10.53391/mmnsa.1400075.

[3] Akhavan Ghassabzade, F., Bagherpoorfard, M. (2024). "Mathematical modeling and optimal control of carbon dioxide emissions". *Control and Optimization in Applied Mathematics*, 9(1), 195-202, doi:https://doi.org/10.30473/coam.2023.67777.1233.

[4] Arditi, R., Ginzburg, L.R. (1989). "Coupling in predator-prey dynamics: Ratio-dependence". *Journal of theoretical biology*, 139(3), 311–326, doi:https://doi.org/10.1016/S0022-5193(89)80211-5.

[5] Bahri, M. (2014). "Stability analysis and optimal harvesting policy of prey-predator model with stage structure for predator". *Applied Mathematical Sciences*, 8(159), 7923–7934, doi:http://dx.doi.org/10.12988/ams.2014.410792.

[6] Beddington, J.R. (1975). "Mutual interference between parasites or predators and its effect on searching efficiency". *The Journal of Animal Ecology*, 44(1), 331–340, doi:https://doi.org/10.2307/3866.

[7] Boulaaras, S., Yavuz, M., Alrashedi, Y., Bahramand, S., Jan, R. (2025). "Modeling the co-dynamics of vector-borne infections with the application of optimal control theory". *Discrete and Continuous Dynamical Systems-S*, 18(5), 1331-1352, doi:https://doi.org/10.3934/dcdss.2024109.

[8] Chakraborty, K., Chakraborty, M., Kar, T.K. (2011). "Bifurcation and control of a bioeconomic model of a prey–predator system with a time delay". *Nonlinear Analysis: Hybrid Systems*, 5(4), 613–625, doi:https://doi.org/10.1016/j.nahs.2011.05.004.

[9] Chakraborty, K., Chakraborty, M., Kar, T.K. (2011). "Optimal control of harvest and bifurcation of a prey–predator model with stage structure". *Applied Mathematics and Computation*, 217(21), 8778–8792, doi:https://doi.org/10.1016/j.amc.2011.03.139.

[10] Clark, C.W. (1974). "Mathematical bioeconomics". In: *van den Driessche, P. (eds) Mathematical Problems in Biology. Lecture Notes in Biomathematics*, vol 2. Springer, Berlin, Heidelberg, doi:https://doi.org/10.1007/978-3-642-45455-4_3.

[11] Collera J.A., Balilo, A.T. (2018). "Dynamics of a delayed intraguild predation model with harvesting". *Symposium on Mathematics (SYMOMATH), Indonesia*, 1937(1), 020006, doi: https://doi.org/10.1063/1.5026078.

[12] Crowley, P.H., Martin, E.K. (1989). "Functional responses and interference within and between year classes of a dragonfly population". *Journal of the North American Benthological Society*, 8(3), 211–221, doi:https://doi.org/10.2307/1467324.

[13] Danane, J., Yavuz, M., Yıldız, M. (2023). "Stochastic modeling of three-species prey–predator model driven by Lévy Jump with mixed Holling-II and Beddington–DeAngelis functional responses". *Fractal and Fractional*, 7(10), 751, doi:https://doi.org/10.3390/fractalfract7100751.

[14] Debnath, S., Majumdar, P., Sarkar, S., Ghosh, U. (2022). "Global dynamics of a prey–predator model with Holling type III functional response in the presence of harvesting". *Journal of Biological Systems*, 30(01), 225–260, doi:https://doi.org/10.1142/S0218339022500073.

[15] Ebrahimipour, M., Mirhosseini-Alizamini, S.M. (2024). "Optimal adaptive sliding mode control for a class of nonlinear affine systems". *Control and Optimization in Applied Mathematics*, 9(2), 123-138, doi:https://doi.org/10.30473/coam.2023.67868.1236.

[16] Eskandari, Z., Naik, P.A., Yavuz, M. (2024). "Dynamical behaviors of a discrete-time prey-predator model with harvesting effect on the predator". *Journal of Applied Analysis and Computation*, 14(1), 283-297, doi:https://doi.org/10.11948/20230212.

[17] Fatima, B., Yavuz, M., Ur Rahman, M.U., Al-Duais, F.S. (2023). "Modeling the epidemic trend of Middle Eastern respiratory syndrome coronavirus with optimal control". *Mathematical Biosciences and Engineering*, 20(7), 11847-11874, doi:https://doi.org/10.3934/mbe.2023527.

[18] Fatima, B., Yavuz, M., Ur Rahman, M.U., Althobaiti, A., Althobaiti, S. (2023). "Predictive modeling and control strategies for the transmission of Middle East respiratory syndrome coronavirus". *Mathematical and Computational Applications*, 28(5), 98, doi:https://doi.org/10.3390/mca28050098.

[19] Ganguli, C., Kar, T., Mondal, P. (2017). "Optimal harvesting of a prey–predator model with variable carrying capacity". *International Journal of Biomathematics*, 10(5), 1750069, doi:https://doi.org/10.1142/S1793524517500693.

[20] Ghosh, B., Pal, D., Legović, T., Kar, T.K. (2018). "Harvesting induced stability and instability in a tri-trophic food chain". *Mathematical Biosciences*, 304, 89-99, doi:https://doi.org/10.1016/j.mbs.2018.08.003.

[21] Gupta, R., Banerjee, M., Chandra, P. (2012). "Bifurcation analysis and control of Leslie–Gower predator–prey model with Michaelis–Menten type prey-harvesting". *Differential Equations and Dynamical Systems*, 20(3), 339–366, doi:https://doi.org/10.1007/s12591-012-0142-6.

[22] Hassell, M., Varley, G. (1969). "New inductive population model for insect parasites and its bearing on biological control". *Nature*, 223(5211), 1133–1137, doi:https://doi.org/10.1038/2231133a0.

[23] Holling, C.S. (1959). "The components of predation as revealed by a study of small-mammal predation of the European Pine Sawfly". *The Canadian Entomologist*, 91(5), 293–320, doi:https://doi.org/10.4039/Ent91293-5.

[24] Jana, S., Guria, S., Ghorai, A., Kar, T.K. (2021). "Complex dynamics of a prey-predator system incorporating functional response dependent prey refuge with harvesting". *Journal of Applied Nonlinear Dynamics*, 10(3), 493–512, doi:https://doi.org/10.1155/2025/354998343.

[25] Joshi, H., Yavuz, M. (2026). "A novel fractional-order model and analysis of cancer-immune system interaction in an avascular environment with an efficient control mechanism". *Journal of Computational and Applied Mathematics*, 473, 116888, doi:https://doi.org/10.1016/j.cam.2025.116888.

[26] Kar, T., Chattopadhyay, S.K. (2010). "A dynamic reaction model of a prey-predator system with stage-structure for predator". *Modern Applied Science*, 4(5), 183, doi:https://doi.org/10.5539/mas.v4n5p183.

[27] Kuang Y., Beretta, E. (1998). "Global qualitative analysis of a ratio-dependent predator–prey system". *Journal of Mathematical Biology*, 36, 389–406. doi:https://doi.org/10.1007/s002850050105.

[28] Lotka, A.J. (1925). "Elements of physical biology". *Nature*, 116, 461, doi:https://doi.org/10.1038/116461b0.

[29] Lv, Y., Zhang, Z., Yuan, R., Pei, Y. (2014). "Effect of harvesting and prey refuge in a prey–predator system". *Journal of Biological Systems*, 22(01), 133–150, doi:https://doi.org/10.1142/S0218339014500089.

[30] Magudeeswaran, S., Vinoth, S., Sathiyanathan, K., Sivabalan, M. (2022). "Impact of fear on delayed three species food-web model with Holling type-II functional response". *International Journal of Biomathematics*, 15(4), doi:https://doi.org/10.1142/S1793524522500140.

[31] Murray, J.D. (2002). "Mathematical biology: I. An introduction (3rd ed.)". *Springer New York, NY*, doi:https://doi.org/10.1007/b98868.

[32] Mustapha, U.T., Maigoro, Y.A., Yusuf, A., Qureshi, S. (2024). "Mathematical modeling for the transmission dynamics of cholera with an optimal control strategy". *Bulletin of Biomathematics*, 2(1), 1-20, doi:https://doi.org/10.59292/bulletinbiomath.2024001.

[33] Nabil, H., Hamaizia, T. (2024). "A three-dimensional discrete fractional-order HIV-1 model related to cancer cells, dynamical analysis and chaos control". *Mathematical Modelling and Numerical Simulation with Applications*, 4(3), 256-279, doi:https://doi.org/10.53391/mmnsa.1484994.

[34] Naik, P.A., Eskandari, Z., Shahkari, H.E., Owolabi, K.M. (2023). "Bifurcation analysis of a discrete-time prey-predator model". *Bulletin of Biomathematics*, 1(2), 111-123, doi:https://doi.org/10.59292/bulletinbiomath.2023006.

[35] Naik, P.A., Eskandari, Z., Yavuz, M., Huang, Z. (2025). "Bifurcation results and chaos in a two-dimensional predator-prey model incorporating Holling-type response function on the predator". *Discrete and Continuous Dynamical Systems-S*, 18(5), 1212-1229, doi:https://doi.org/10.3934/dcdss.2024045.

[36] Naik, P.A., Eskandari, Z., Yavuz, M., Zu, J. (2022). "Complex dynamics of a discrete-time Bazykin–Berezovskaya prey-predator model with a strong Allee effect". *Journal of Computational and Applied Mathematics*, 413, 114401, doi:https://doi.org/10.1016/j.cam.2022.114401.

[37] Nkeki, C., Mbarie, I.a. (2025). "On a mathematical model and the efficacy of control measures on the transmission dynamics of chickenpox". *Bulletin of Biomathematics*, 3(1), 37-61, doi:https://doi.org/10.59292/bulletinbiomath.1707079.

[38] Panja, P. (2021). "Dynamics of a predator–prey model with Crowley–Martin functional response, refuge on predator and harvesting of super–predator". *Journal of Biological Systems* 29(03), 631–646, doi:https://doi.org/10.1142/S0218339021500121.

[39] Perko, L. (2013). "Differential equations and dynamical systems". *Springer New York, NY*, doi:https://doi.org/10.1007/978-1-4613-0003-8.

[40] Safuan, H.M., Musa, S.B. (2016). "Food chain model with competition interaction in an environment of a biotic resource", *23rd Malaysian National Symposium of Mathematical Sciences (SKSM23), Malaysia*, 1750, 030015, doi:https://doi.org/10.1063/1.4954551.

[41] Safuan, H.M., Sidhu, H., Jovanoski, Z., Towers, I. (2013). "Impacts of biotic resource enrichment on a predator–prey population". *Bulletin of mathematical biology*, 75(10), 1798–1812, doi:https://doi.org/10.1007/s11538-013-9869-7.

[42] Samanta, S., Chattopadhyay, J. (2013). "Effect of kairomone on predator–prey dynamics—A delay model". *International Journal of Biomathematics*, 6(5), doi:https://doi.org/10.1142/S1793524513500356.

[43] Sen, M., Banerjee, M., Morozov, A. (2012). "Bifurcation analysis of a ratio-dependent prey–predator model with the Allee effect". *Ecological Complexity*, 11, 12-27, doi:https://doi.org/10.1016/j.ecocom.2012.01.002.

[44] Singh, M.K., Poonam, P. (2025). "Bifurcation analysis of an additional food-provided predator-prey system with anti-predator behavior". *Mathematical Modelling and Numerical Simulation with Applications*, 5(1), 38-64, doi:https://doi.org/10.53391/mmnsa.1496827.

[45] Shang, Z., Qiao, Y., Duan, L., Miao, J. (2021)." Bifurcation analysis in a predator–prey system with an increasing functional response and constant-yield prey harvesting. *Mathematics and Computers in Simulation*, 190, 976-1002, doi:https://doi.org/10.1016/j.matcom.2021.06.024.

[46] Valinejad, A., Babaei, A., Zarei, Z. (2024). "An adaptive time-stepping algorithm to solve a stochastic Lotka-Volterra competition system with time-variable delays". *Control and Optimization in Applied Mathematics*, 9(2), 187-199, doi:https://doi.org/10.30473/coam.2024.67940.1237.

[47] Vinoth, S., Sivasamy, R., Sathiyanathan, K., Grienggrai Rajchakit, G., Hammachukiattikul, P., Vadivel, R., Gunasekaran, N. (2021). "Dynamical analysis of a delayed food chain model with additive Allee effect. *Advances in Difference Equations*, 54(2021), doi:https://doi.org/10.1186/s13662-021-03216-z.

[48] Vinoth, S., Sivasamy, R., Sathiyanathan, K., Unyong, B., Vadivel, R., Gunasekaran, N. (2022). "A novel discrete-time Leslie–Gower model with the impact of Allee effect in predator population". *Complexity*, 2022(1), doi:https://doi.org/10.1155/2022/6931354.

[49] Volterra, V. (1926). "Fluctuations in the abundance of a species considered mathematically". *Nature*, 118, 558-560, doi:http://dx.doi.org/10.1038/118558a0.